GNC 2014: 9th International ESA Conference on Guidance, Navigation & Control Systems
Porto, Portugal | 2 - 6 June 2014
European Space Agency

TARGET RELATIVE NAVIGATION PERFORMANCE RESULTS FROM SINPLEX: A MINIATURIZED NAVIGATION SYSTEM

S. Steffes[1] (stephen.steffes@dlr.de), S. Theil[1], M. Dumke[1], D. Heise[1], H. Krüger[1], M. Sagliano[1], M. Samaan[1], H. Oosterling[2], E. Boslooper[2], T. Duivenvoorde[2], J. Schulte[3], S. Söderholm[3], D. Skaborn[3], Y. Yanson[4], M. Esposito[4], S. Conticello[4], R. Visee[5], B. Monna[5], F. Stelwagen[5]
[1]DLR German Aerospace Center, Institute of Space Systems, Robert-Hooke-Str. 7, 28359 Bremen, Germany.
[2]TNO, PO box 155, 2600AD Delft, Netherlands.
[3]ÅAC Microtec AB, Uppsala Science Park, Dag Hammarskjölds väg 48, 75183 Uppsala, Sweden.
[4]cosine Research B.V., J.H. Oortweg 19, NL-2333 CH Leiden, Netherlands.
[5]SystematIC design B.V., Motorenweg 5G, 2623 CR Delft, Netherlands.

ABSTRACT

The goal of the SINPLEX project is to develop an innovative solution to significantly reduce the mass of the navigation subsystem for exploration missions which include landing and/or rendezvous and capture phases. The system mass is reduced by functionally integrating the navigation sensors, using micro- and nanotechnology to miniaturize electronics and fusing the sensor data within a navigation filter to improve navigation performance. A breadboard system was built and includes a navigation computer, IMU, laser altimeter/range finder, star tracker and navigation camera. This system was tested at short distances with realistic trajectories in DLR's TRON testbench. This paper covers an overview of the hardware and testbench and presents performance results from the hardware-in-the-loop tests.

1. INTRODUCTION

For space missions which land on other celestial bodies, modernizing and miniaturizing the navigation subsystem is an important objective. In particular, [1] suggests that the most useful technologies would be miniaturized star trackers, laser altimeters and functionally integrating multiple GNC components, all of which is addressed by the SINPLEX (Small Integrated Navigation system for PLanetary EXploration) relative navigation system. The main goal of the SINPLEX project is to develop an innovative navigation system for exploration missions which include a landing and/or a rendezvous and capture/docking phase with a mass which is significantly lower than conventional systems. Reducing mass while maintaining good navigation performance is achieved by functionally integrating different sensors, utilizing micro- and nanotechnologies to miniaturize electronics and combining sensor measurements using sensor hybridization approaches to improve the performance of the complete navigation subsystem.

Within the project a breadboard system was produced, which includes an inertial measurement unit (IMU), star tracker (STR), navigation camera, laser altimeter/range finder (LA), navigation computer (NC) and power distribution unit. The system was designed to meet the combined requirements needed for a general Moon landing, asteroid landing and sample container rendezvous/capture mission scenario [2]. Hardware-in-the-loop (HIL) testing was done at DLR's TRON (Testbed for Robotic Optical Navigation) facility [3] to measure its navigation performance and demonstrate its applicability for object relative autonomous navigation in space applications. More information about the SINPLEX project can be found at our website: `http://www.sinplex.eu` and in previous papers [2,4--6]. SINPLEX is a research and development project funded by the European Commission under the 7th Framework Programme (grant ID 284433).

This work provides an overview of the final design of the manufactured breadboard system as background and the final performance results from the HIL tests. The paper starts by describing the breadboard design and the onboard navigation algorithms. The HIL test bench is presented, including the test trajectories used. Testing of the breadboard is limited to close range terrain relative tests. Finally, performance results are shown.

Table 1: *Properties of each optical sensor.*

Specification	Navigation Camera	STR Camera	LA Receiver
Rectangular FOV	$40deg$	$16 \times 20deg$	$3.2mrad$
Entry aperture diameter	$10mm$	$10 \times 30mm$ elliptical	$10mm$
Sensor	HAS2	HAS2	Sensl PCDMini-00020
Spectral range	$40-800nm$	$40-800nm$	$532nm$
Sensor size (active)	$1024 \times 1024pixels$	$472 \times 712pixels$	$1pixel$
Pixel size	$18\mu m$	$18\mu m$	$20\mu m$

Table 2: *Mass breakdown for breadboard.*

Component	Mass [kg]
Housing	1.5
Power Distribution Unit	0.04
NC	0.03
IMU Subsystem	0.06
LA Subsystem	0.9
Camera Electronics	0.18
Misc.	0.39
Total	3.1

Table 3: *Power breakdown for breadboard.*

Component	Power [W]
Power Distribution Unit	0.3
NC	2.5
IMU Subsystem	1.0
LA Subsystem	5.5
2x Camera Subsystem	7
Total	16.3

2. BREADBOARD DESIGN

The SINPLEX flight model design (shown in Fig. 1 and Fig. 2 with specifications listed in Table 1) is a highly integrated, fully redundant, miniaturized, autonomous navigation system. The system features a suit of redundant components, each chosen to fulfill the performance requirements with minimal mass. A breadboard version was produced with non-redundant subsystems to demonstrate the technology. The mass and power breakdowns in Table 2 and Table 3 represent measured values from the built breadboard system and do not include redundant components. The overall volume is roughly $17 \times 21 \times 20cm$. The flight model and breadboard are described in detail in [2, 5].

The IMU uses four MEMS accelerometers (Colibrys MS9002) and gyros (Analog Devices ADXRS646BBGZ) in a tetrahedral configuration. The main IMU electronics board samples the sensors at 100Hz, corrects for known errors and integrates the data at high rate as part of the navigation filter.

The LA provides target range by statistically measuring the time of flight of a high frequency pulsed 532nm laser (Teem Photonics MNG-03E). A single photon avalanche diode (Sensl PCDMini-00020) measures single received photons. The system has an expected range up to $10km$.

The navigation camera provides images of the target surface, which are processed to measure feature positions, depending on the mission scenario. A lens barrel forms the receiving optics for both the navigation camera and LA receiver. The green light for the LA is split out by a notch reflection filter and exits the lens barrel through a hole on the side. The remainder of the light goes to the navigation camera detector. Images are processed on a custom FPGA board and the resulting measurements are sent to the NC.

The STR images are processed by a custom FPGA board (same design as the navigation camera FPGA board) and the design is based on the Multiple Aperture Baffled Star Tracker [7].

The NC hosts the navigation algorithm and controls all sensor scheduling and data passing between components using the SPA-1 (Space Plug and Play Avionics) protocol. The NC outputs a navigation solution (vehicle position, velocity and attitude) in real-time at $10Hz$ during every mission phase. Processing of sensor measurements is distributed over all the components to offload much of the computational burden from the NC, allowing for lighter loads on the NC processor and communications bus.

The navigation algorithm on the breadboard computes both inertial and terrain relative navigation states. A delayed error state extended Kalman filter (EKF) similar to [8, 9] is used to fuse the sensor measurements, which include: acceleration and angular rate from the IMU, inertial attitude from the STR, terrain relative distance from the LA and terrain relative feature positions (bearing only) from the navigation camera. The terrain relative position is found by

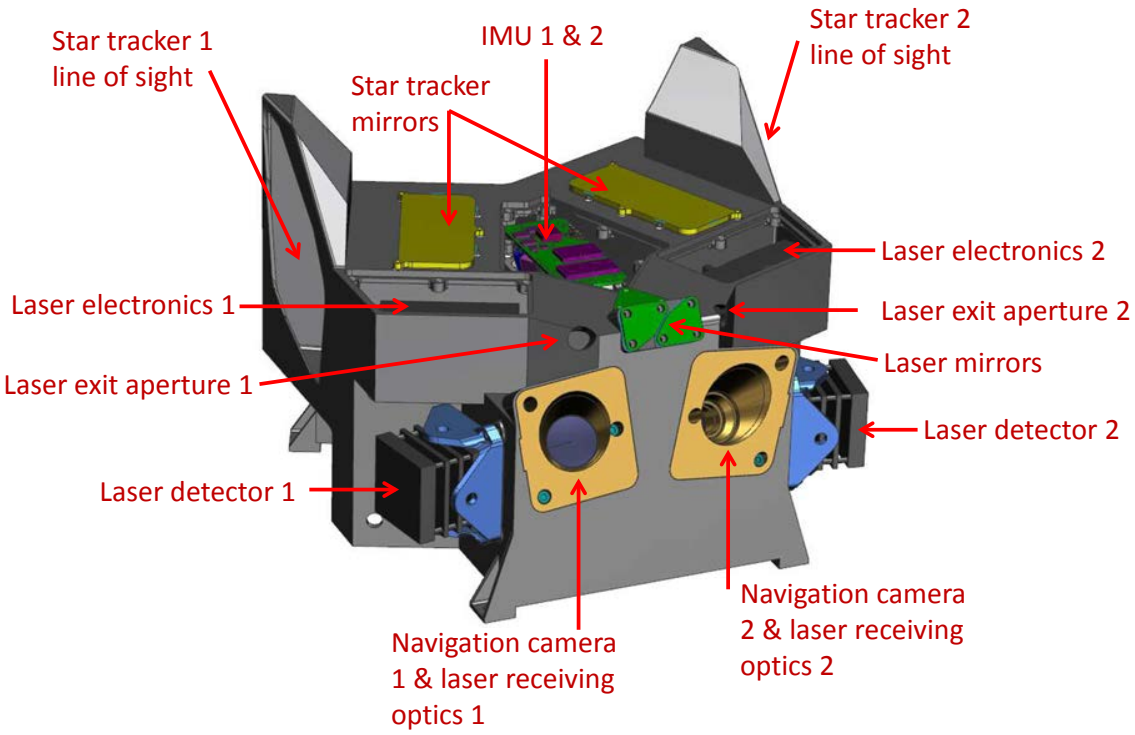

Fig. 1: *Front-top view of SINPLEX flight model with cover plates removed.*

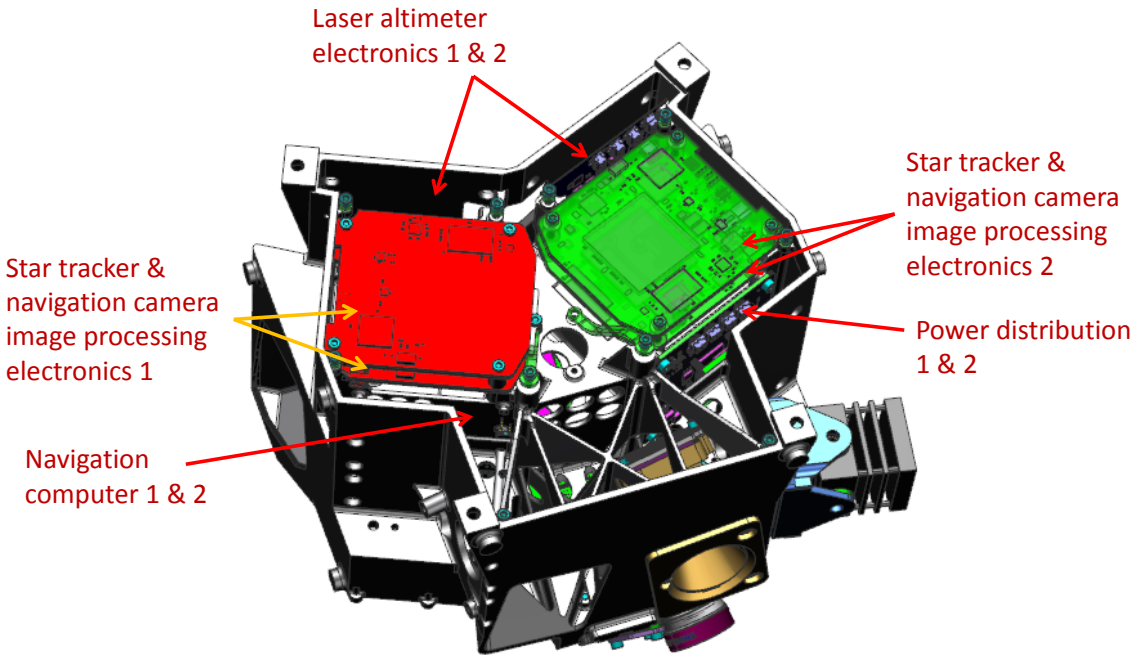

Fig. 2: *Bottom view of SINPLEX flight model with cover plates and some components removed.*

tracking up to four features over time using a variant of EKF-SLAM [10]. Using the filter, this provides updates to the inertial velocity and attitude states since any change in velocity or attitude affects the movement of the features in the image.

The navigation software is distributed over several subsystems and at three separate rates. Image processing algorithms are run on the camera FPGAs and only the final measurement results are sent to the NC. Raw and compensated IMU measurements are processed within the IMU subsystem, which uses the $100Hz$ high-rate (HR) navigation algorithm to provide $10Hz$ integrated delta-velocity and delta-angle increments to the NC, which are compensated for any rotations over the interval. Raw LA measurements are processed within the LA subsystem and range measurements are sent to the NC. There are two additional algorithms that are run directly on the NC: the navigation medium-rate (MR) and low-rate (LR) tasks. The MR task runs at $10Hz$ and is responsible for integrating the equations of motion, calibrating clocks and calculating the state transition matrix for the EKF. The LR task runs at $1Hz$ and is responsible for propagating the EKF with the state transition matrix and updating the EKF with the LA and image processing measurements. State corrections from the LR task are sent to the MR task to correct the navigation state. IMU error estimates (sensor biases and scale factors) are sent from the MR task to the HR task to compensate the integrated IMU measurements. A similar 2-rate approach was successfully used for the Hybrid Navigation System experiment [8], which allows for an optimal filter, reduced real-time constraints and the processing load to be spread out over time.

3. HARDWARE-IN-THE-LOOP SETUP

Terrain relative navigation tests are done in the TRON laboratory [3]. The SINPLEX breadboard is mounted to the end of a 7-DOF (degrees of freedom) robotic arm (Fig. 3) which can move along a $10.5m$ track. The robot can then be precisely positioned in real-time using a dSPACE real-time simulator (a modular COTS real-time simulation platform) and can automatically run through any programmed trajectory, within the limits of the robot. Several 3D terrain models are present in the lab on 3 of the walls, which represent scaled Moon and asteroid landscapes. A sample return container model and a complete 3D scaled asteroid model are also available. A 5-DOF lamp and gantry system provide uniform lighting in a programmed direction and path. Fig. 4 shows the breadboard attached to the robot and all the additional hardware components needed for HIL testing.

TRON can also provide an accurate measurement of the run trajectory by tracking the breadboard with a laser tracker (AT901-MR from Lecia). A T-Mac device is rigidly attached to the breadboard, which can be tracked by the laser tracker in 6-DOF. The position and attitude alignment between the T-Mac and navigation camera is measured by tracking the T-Mac with the laser tracker while the navigation camera views an optical calibration target in various poses. With this, the reference trajectory from the laser tracker can be transformed into the reference trajectory of the navigation camera. This provides an accurate reference trajectory to compare with the navigation data from the breadboard.

A Jenoptik Optical Sky field Simulator (OSI) stimulates optical camera systems for observing objects with an optically finite distance. It mainly consists of an optical head, which projects the image, and a control computer including remote interface software. The optical head includes a micro display with $800 \times 600 pixel$ resolution and is inserted into the STR baffle with a special adapter. The OSI host PC receives attitude commands remotely from the dSPACE system. The PC calculates and projects a simulated image of the sky (including stars, planets, the Moon, single event upsets, etc.) through the optical head as a collimated beam. The beam enters the camera, the NC triggers the camera, and the STR processes the captured image. Optical distortions in the STR image caused by the OSI orientation are calibrated and compensated in the STR and NC software.

For these tests a RaspberryPi is additionally attached to the breadboard to provide an interface for the subsystems to output debugging information remotely to the user. This is data which would otherwise not be accessible to the user. The RaspberryPi is only used for this purpose and is otherwise not needed for HIL testing.

Two main trajectories were used to test the breadboard in TRON. For all HIL tests, the full SINPLEX system is used to navigate through the TRON lab. The navigation camera takes images of the terrain models, the LA measures the distance to the terrain and the IMU measures the dynamics of the robot. There are no stars within the lab, so the STR is stimulated with the OSI, which shows sky field images which agree with the commanded robot motion. Fig. 5 shows the trajectories plotted in the TRON reference frame. In both trajectories the robot mainly moves along the $+y$ TRON axis and the $+z$ TRON axis points upwards. The lighting of the lab is configured in order to provide good feature qualities for the feature tracker.

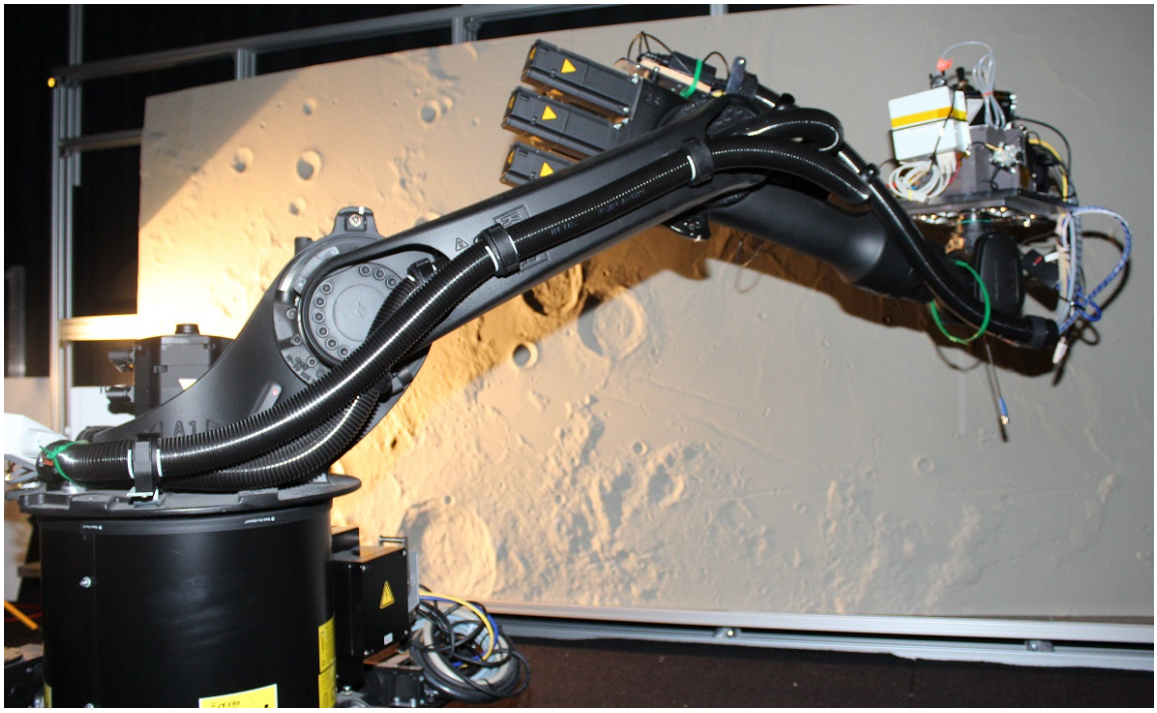

Fig. 3: *SINPLEX breadboard attached to TRON robotic arm.*

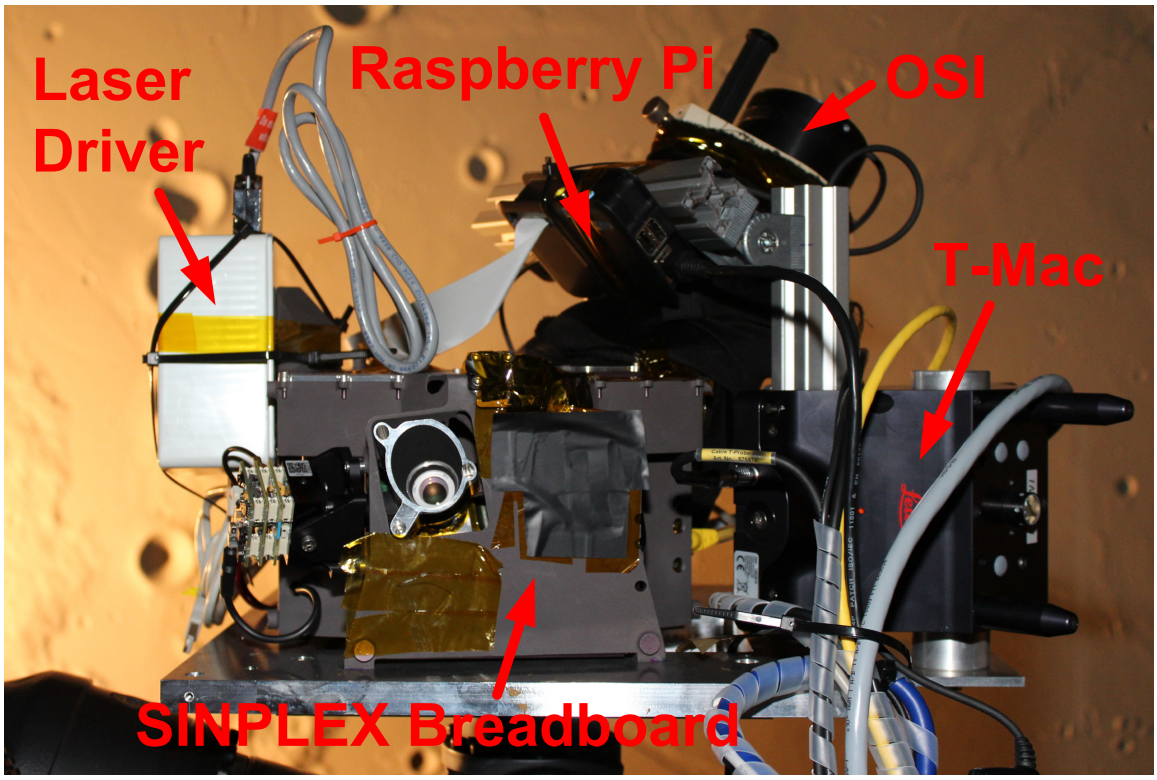

Fig. 4: *Additional hardware components attached to breadboard for HIL testing.*

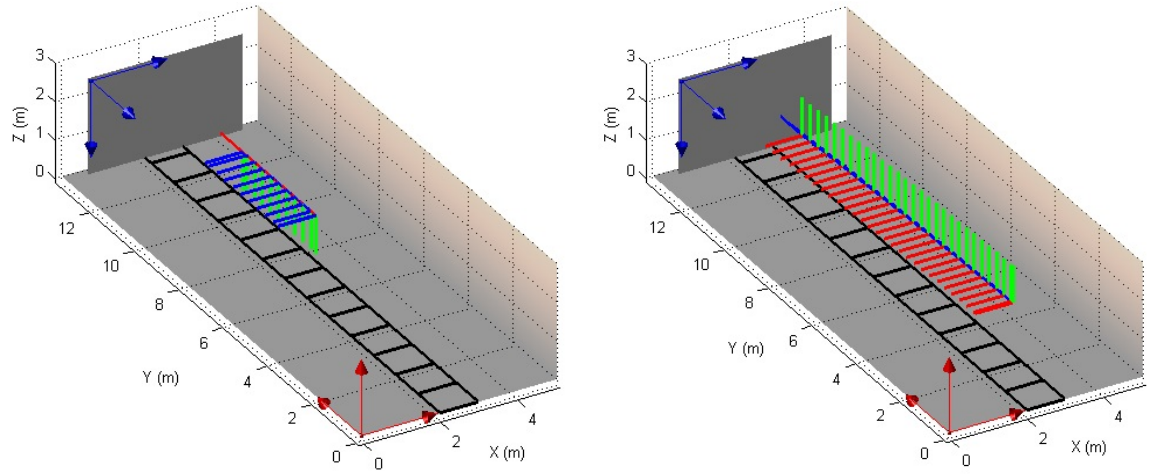

(a) (b)

Fig. 5: *3D view of the lateral (a) and asteroid landing (b) trajectories in the TRON reference frame. The navigation camera axes are shown at several points along the trajectory. The imaging axis points parallel to the blue axis.*

The first trajectory simulates a part of a lunar descent orbit. The navigation camera is pointed towards one of the terrain models (on the left ($x = 0m$) or right ($x = 5m$) wall) and starts near the $y = 0m$ side of the lab. The robot then moves laterally over the terrain at a constant velocity and constant x and z position. Fig. 5(a) shows the trajectory which points towards the left terrain. The trajectory for the right terrain is the mirror opposite but goes the full length of the wall. The left terrain model only covers half of the wall. The lab is not long enough to simulate more than a small portion of an orbit, so the same trajectory is used with different velocities to simulate several small portions of the overall orbit. This trajectory provides camera inputs which are representative of a real lunar descent orbit with laboratory lighting, but the measurements from the LA and IMU will reflect the actual lab scale and robot dynamics.

The second trajectory (Fig. 5(b)) models the last $10m$ of a trajectory with lands on a small asteroid ($1km$ diameter, $5e11kg$, spherical, C type, 7hr rotation period). The breadboard starts near the $y = 0m$ side of the lab and the navigation camera is pointed towards the terrain model at the far end of the lab ($y = 13m$). The BB is driven along the y-axis towards the terrain starting with a velocity of $0.13m/s$ and accelerating up to $0.135m/s$ at the end. Simultaneously, the BB is moved in the $-x$ TRON direction starting at $0.002m/s$ and ending at $0.007m/s$. The attitude of the BB is constant throughout the trajectory and the navigation camera always points towards the terrain. This trajectory accurately models all of the translational dynamics and terrain relative distances. However, it is run under Earth gravity and the laboratory lighting. Nevertheless, it is a good representative trajectory.

4. RESULTS

The breadboard system went through extensive sensor and system level testing and some results are presented here. These are the results at the end of the SINPLEX project. Additional tests cannot be carried out due to a lack of time within the project plan. A number of improvements and further development are being considered for the next generation of the system.

The breadboard was first tested on a sensor level to characterize the individual sensor performances. The IMU was calibrated and characterized with a rotation table. The LA was compared against a more accurate reference measurement. The feature tracker measurements were compared against known camera position and orientation changes. The STR was compared against the simulated sky field image. The resulting single sensor performance values listed in Table 4 are compared with the expected values calculated from the specifications of the individual components and algorithms used. These results show that the sensors behaved well (except for the STR which sufferred from a misalignment in one component) and that there is still some improvements which can be made. To that effect, a number of possible software and hardware enhancements have already been identified which may be used in the next generation of the SINPLEX system. The effects of these sensor performances on the overall system performance can be seen below.

Table 4: *Single sensor performances.*

Measurement	Expected 3σ Performance	Measured 3σ Performance
Accelerometer Bias $[mg]$	10	2.5
Gyro Bias $[deg/hr]$	360	140
LA Range $[cm]$	12	12.7
Feature Tracking $[pixel]$	0.7	0.94
Star Tracker $[deg]$	0.003	0.18

Table 5: *List of runs done with the lateral trajectory.*

Terrain Model	Velocity $[m/s]$	Mean TR Distance $[m]$	Number of Runs	Color Coding
Left	0.0733	3.75	2	blue
Left	0.1459	3.75	3	green
Left	0.733	3.75	2	red
Right	0.0734	3.53	1	cyan
Right	0.1455	3.53	1	magenta
Right	0.2941	3.53	7	yellow

The full breadboard system was tested using both the lateral and asteroid trajectories. Several runs for each trajectory were done and the results are compiled here. The system was initialized assuming perfect knowledge of position, velocity and attitude. This was followed by a $30sec$ period of no motion when the navigation algorithm directly measures its accelerometer and gyro biases. The trajectory then starts and ends when the robot reaches the end of the terrain model.

The navigation algorithm cannot improve the initial absolute position estimate since no sensor measurements provide this information, but it can prevent the position from drifting over time by using the feature estimates. Absolute and terrain relative (TR) velocity are the same thing since the navigation state is estimated in a surface fixed reference frame, which can be directly observed by tracking features. Inertial attitude estimation is maintained using the STR results. Without the STR the navigation algorithm cannot improve the inertial attitude estimate, but it can prevent the attitude from drifting over time by using the feature estimates. The navigation algorithm tracks 4 features throughout the trajectory, which may change if the feature tracker fails to re-find the feature. These 4 features plus the LA measurement can be fit to a plane, which then represents a rough model of the target surface. The error in the distance and angle of this feature plane is one measure of the accuracy of the feature estimates. Note that SINPLEX was not designed to accurately measure the TR attitude. However, it is something that can be measured with the system and may be important for some potential missions.

A. LATERAL TRAJECTORY

Fig. 6 shows the navigation performance results for the lateral trajectory runs. Errors are calculated by comparing the breadboard's navigation solution to the reference trajectory from the laser tracker. The plots show the results from 16 individual runs which are listed in Table 5. Runs with faster velocities have shorter final trajectory times since the trajectory always runs over the full length of the terrain model. These runs fall within the range of scaled velocities for a lunar $100km \times 10km$ descent orbit. However, there are a number of differences between the HIL trajectory and the actual lunar orbit scenario which make it difficult to be able to give any meaning to this comparison. Even if the performance in the HIL trajectory doesn't meet the desired performance requirement, it still doesn't mean that the requirement would not be met in a more representative trajectory. Therefore, the scaled system requirements are not shown.

The only results that can be compared to a mission requirement are the inertial attitude errors, since these are not affected by trajectory scaling. Fig. 6(b) shows that the attitude error regularly exceeds the requirement of $0.3deg$ 3σ. This is not surprising considering the poor STR sensor performance.

The rest of the data show that the filter is behaving correctly: errors do not grow unbounded and show the same trend across runs. There are a number of outlying runs which have errors significantly different than the general trends. These can typically be contributed to errors in the feature tracker, which are larger than

expected but not large enough to exceed the sanity checks in the filter. The feature tracker errors are largely due to poor lighting within TRON and the lack of an automatic image exposure time algorithm in the navigation camera subsystem, both of which can be improved in the next generation of the system.

Features are found on-line and do not correspond to any precalculated landmarks on the target. It is only known that the true feature location lies somewhere on the target surface (which is approximately a plane with 10*cm* surface roughness). Some measure of the feature position accuracy can be obtained by fitting the estimated feature positions to a plane and then comparing the distance and orientation of this plane to the true target surface. Fig. 6(c) and Fig. 6(d) show the errors in the estimated feature plane, calculated by comparing to the true terrain surface plane. Before the trajectory starts the feature plane errors are small and stable. After the trajectory starts these errors increase and vary greatly. Feature plane attitude estimation is greatly dependent on the spread of the features over the image. The navigation algorithm is tuned to put a larger weight on distance accuracy than attitude accuracy. The algorithm chooses features spread over the inner part of the image so the LA measurement has a higher weighting when estimating the feature distance. This causes poor feature plane attitude estimation since the features are grouped close together. The large variation of the feature plane distance error is likely a result of poor feature tracking performance due to the contrast changes in the image throughout the trajectory. Some image normalization is done online for the navigation camera images, but the camera integration time (shutter time) is constant throughout the trajectory.

B. ASTEROID TRAJECTORY

Fig. 7 shows the navigation performance results for the asteroid trajectory runs. Errors are calculated by comparing the breadboard's navigation solution to the reference trajectory from the laser tracker. The plots show the results from 10 individual runs, which each have a different color in order to distinguish between runs. The thick dashed black line is the combined 3σ value for all runs. The thick dashed red line is the 3σ requirement value which the system was built to meet.

The dynamics for these runs are the same as a general asteroid landing trajectory, except with Earth gravity. Therefore, the results can be compared with the system performance requirements, but any errors due to the accelerometers will degrade the performance unrealistically since there are no thrusting maneuvers for this part of the trajectory and the accelerometers would not be used.

Fig. 7(a) shows very good velocity performance that almost meets the requirements. There are a couple of outlying runs, which significantly raise the 3σ error near 10*s* and 20*s* and fails the requirement. The most significant errors from these runs come from large errors in feature tracking measurements, which is likely due to poor image contrast.

Fig. 7(b) shows similar performance as Fig. 6(b). This is not surprising since the attitude rates are the same for both trajectories.

Fig. 7(c) shows that the feature plane distance error exceeds the requirement soon after the trajectory starts. The data suffers from a timing error which causes the distance error to increase when the BB is moving. Removing this effect would reduce the error and bring the system closer to meeting the requirement.

Fig. 7(d) shows that the feature plane attitude error is significantly large during the middle of the trajectory (40 to 55*s*). Data from the FT shows that the image quality is the worst around this point, which causes excessive error in the FT measurements. This could account for a significant portion of this angular error. Tracking additional features would also reduce this error, which would be possible with a more powerful navigation computer.

5. SUMMARY

SINPLEX has the potential to be a powerful navigation system technology with significant mass savings compared to a suit of COTS components with similar performance. The produced breadboard model has been through extensive testing and the hardware-in-the-loop results for a lateral terrain relative trajectory and an asteroid landing trajectory show promising results. Although some results violate the requirements to which the system was designed, it is very likely that the next generation of the system will have greatly improved performance by addressing the various issues and improvements which have already been identified in the breadboard.

REFERENCES

[1] Cornelius J. Dennehy. Some U.S. Perspectives on Miniaturized Guidance , Navigation & Control (GN&C) Hardware Components. Presentation at ESA Workshop on Avionics Data, Control, and Software Systems (ADCSS), October, 2012.

[2] Stephen R Steffes and et. al. SINPLEX: a Small Integrated Navigation System for Planetary Exploration. In *36th Annual AAS Guidance and Control Conference*, Breckenridge, Colorado, February 2013. AAS. AAS 13-043.

[3] H. Krüger and S. Theil. TRON-hardware-in-the-loop test facility for lunar descent and landing optical navigation. In *18th IFAC Symposium on Automatic Control in Aerospace*, 2010.

[4] Erik Laan and et. al. SINPLEX: A Small Integrated Navigation System for Planetary Exploration. In *64th International Astronautical Congress*, Beijing, China, September 2013. IAC. IAC-13,C1,4,6,x17804.

[5] Stephen R Steffes and et. al. Target Relative Navigation Results from Hardware-in-the-Loop Tests Using the SINPLEX Navigation System. In *37th Annual AAS Guidance and Control Conference*, Breckenridge, Colorado, February 2014. AAS. AAS 14-402.

[6] Simon Conticello and et. al. Development and test results of sinplex, a compact navigator for planetary exploration. In *4S Symposium*, Majorca, Spain, May 2014.

[7] Johan Leijtens and et. al. A New Star (Sensor) is Born. In *Proceedings of the International Conference on Space Optics*, Rhodes, Greece, October 2010. ICSO.

[8] Stephen R. Steffes. Real-Time Navigation Algorithm for the SHEFEX2 Hybrid Navigation System Experiment. In *Proceedings of the AIAA Guidance, Navigation, and Control Conference*, Minneapolis, Minnesota, August 2012. AIAA. AIAA-2012-4990.

[9] Stephen R Steffes. Computationally distributed real-time dual rate kalman filter. *AIAA Journal of Guidance, Control and Dynamics*, 2014.

[10] Hugh Durrant-Whyte and Tim Bailey. Simultaneous Localization and Mapping: Part I. *IEEE Robotics & Automation Magazine*, pages 99--108, June 2006.

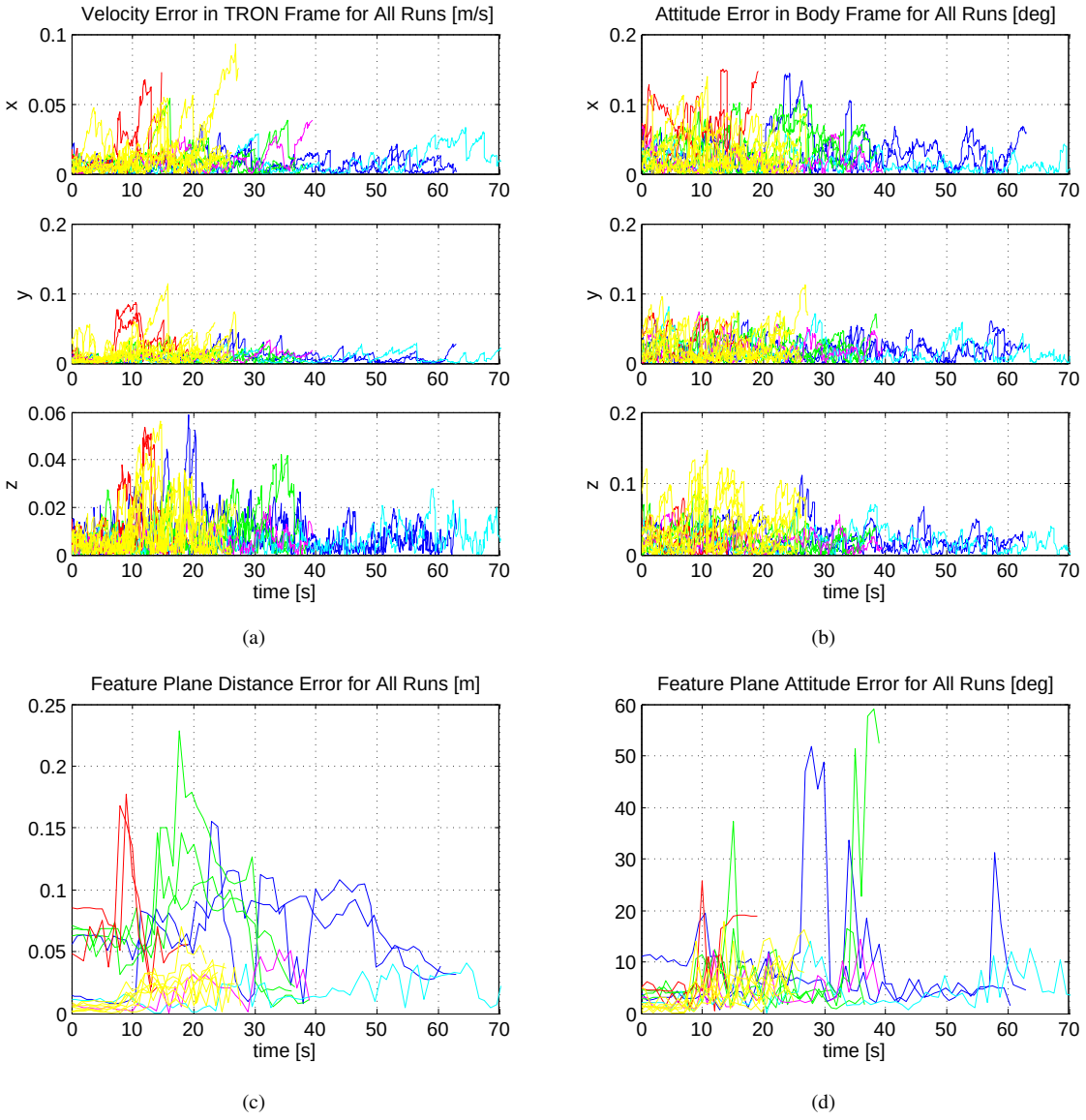

Fig. 6: *Results from lateral trajectory test (see Table 5 for color coding). (a) TR velocity error. (b) Inertial attitude error. (c) Feature plane distance error. (d) Feature plane attitude error.*

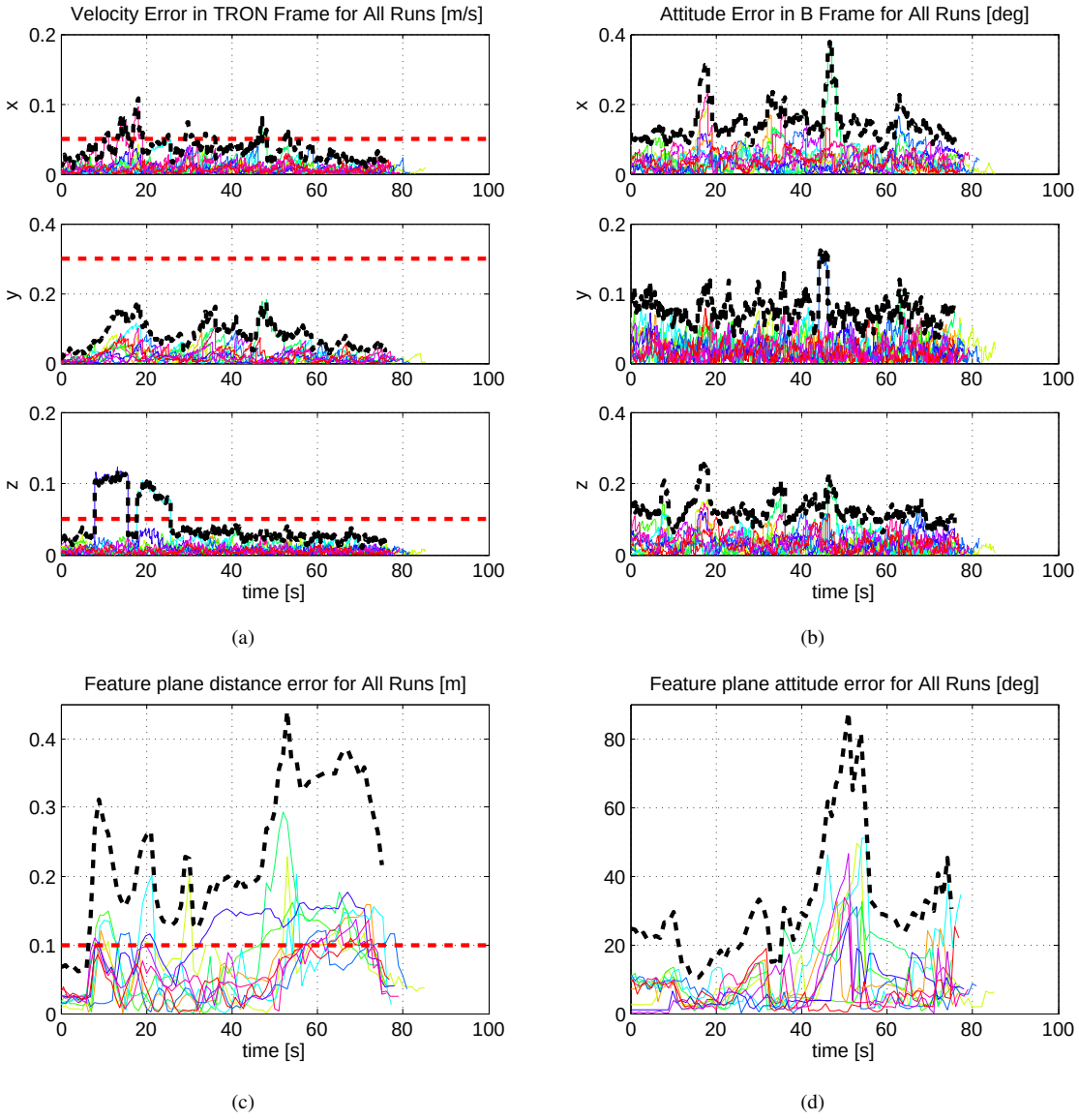

Fig. 7: *Results from asteroid trajectory test (see text for color coding). (a) TR velocity error. (b) Inertial attitude error. (c) Feature plane distance error. (d) Feature plane attitude error.*